

# Spectral Response of Multispectral Sensors to Remote Sensing Based PM10 Retrieval

<sup>[1]</sup> Ajay N Roy, <sup>[2]</sup> Anjali G. Jivani, <sup>[3]</sup> Bhuvan S. Parekh

<sup>[1]</sup> Department of MCA, <sup>[2]</sup> Department of Computer Science

<sup>[1]</sup> D. D. University, Nadiad, India, <sup>[2]</sup> The Maharaja Sayajirao University of Baroda, Vadodara, India

**Abstract** - The spectral characteristics are a key to remote sensing applications. The extraction of meaningful information from the imagery necessitates good knowledge and understanding of the spectral characteristics of the satellite sensors. Multispectral satellite sensors record information in wide of spectral channels. The spectral response in specific wavelength plays a major role in remote sensing applications. PM10 estimation using remote sensing is now becoming popular approach for pollution monitoring. Several approaches have been used for estimation of PM10 using various satellite sensors. This paper presents the sensitivity of satellite sensors at different wavelengths and its application to estimate PM10. The atmospheric absorption, reflectance and transmission behavior for Visible and Infrared ranges is a key to particulate matter monitoring. The sensitivity of different channels of MODIS, MERIS, SPOT5, Landsat TM/ETM+ and Landsat 8 have been analyzed. The sensor characteristics have also been presented to find the suitability of these sensors for PM10 distribution.

**Key Words**— Landsat, MERIS, MODIS, PM10, Spectral response, SPOT5.

## I. INTRODUCTION

Highlight a section that you want to designate with a certain Respirable Suspended Particulate Matter (RSPM) also known as particulate matter 10 (PM10) are particles with size less than 10 microns [1] [2]. Ground station based monitoring of PM10 cannot provide distribution mapping of an area as the concentration is highly variable. Remote sensing is an effective approach for mapping the PM10 distribution [3] [4].

The remote sensing sensors can be categorized into active and passive sensors. Passive sensors need an external source of energy, which is normally given by the sun which is the natural source of energy [5]. The reflected and emitted energy from the target object is detected by the satellite sensors. Active sensors have their own source of energy. The transmission of energy from the surface is recorded by the sensors for different portion of the electromagnetic spectrum including both visible and non-visible regions of the spectrum [6]. Transmissivity is the ability of the atmosphere to allow the energy to pass through it. It depends on the wavelength and type of radiation. The atmospheric gases allow energy with certain wavelength to pass through, whereas absorbs certain wavelength energy. In certain range of EM spectrum, there is very little or no absorption of energy, which allows the energy to easily pass through the atmosphere.

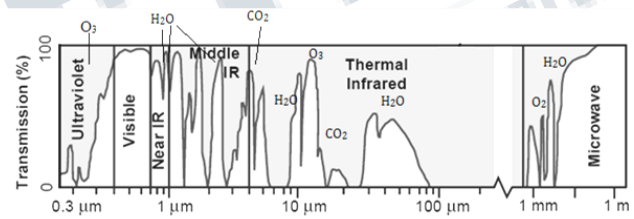


**Fig. 1 Atmospheric Windows in EM ranges\***

\*Source: Randall B. Smith, Introduction of Remote Sensing of Environment, 2012, TNTmips microimages.com

These wavelength ranges are known as atmospheric windows and records the best energy values to acquire the information about the phenomena of the earth. Atmospheric windows are present in the visible part (0.4  $\mu\text{m}$  - 0.76  $\mu\text{m}$ ) and the infrared regions of the EM spectrum [7] [11].

In the UV (0.25 - 0.4  $\mu\text{m}$ ) and visible (0.4-0.7  $\mu\text{m}$ ) range of wavelengths, the sun energy and its reflected light dominates the radiance being emitted back to the space. Very few gases (O<sub>3</sub>, SO<sub>2</sub>, NO<sub>2</sub>, formaldehyde and glyoxal) exist that have absorption features that allow their detection at UV and visible wavelengths [12] [13]. Aerosols dominate visible radiative transfer. Particulate Matter can be recognized using visible wavelength, because light scattering by aerosols is strongly dependent

on the wavelength of light. Also when the particle size and wavelength becomes equal, there is highest mie scattering [12].

Atmospheric absorption in infrared (IR) region is mainly due to water vapor (H<sub>2</sub>O) and carbon dioxide (CO<sub>2</sub>) molecules, which occurs in absorption bands centered at the wavelengths from NIR to long wave IR (0.7 to 15  $\mu$ m). Most of the radiation is absorbed by the atmosphere in far infrared region. (Ali, 2010). The emitted thermal IR have atmospheric windows in shortwave TIR (3.5- 5  $\mu$ m) and longwave TIR (8-14  $\mu$ m) electromagnetic region [14] [15].

## II. SPECTRAL RESPONSE OF SATELLITE SENSORS

The wavelengths for remote sensing applications can be defined by comparing the characteristics of the radiation and energy with the atmospheric windows available for the satellite sensor [8]. The first part of the paper describes the wavelength of selected sensors and their sensitivity for PM<sub>10</sub> estimation using few PM<sub>10</sub> retrieval approaches. In the end, the results of our work done based on atmospheric correction approach have been discussed with specific reference to wavelength and channel sensitivity for Landsat ETM+ sensor. MODIS, MERIS, SPOT5 and Landsat TM/ETM+ and Landsat 8 satellite sensors have been selected and their few research outcomes have been analyzed [8].

### A. MODIS

There exists a direct relationship between the atmospheric particles and satellite-derived Aerosol Optical Depth (AOD) because AOD represents the quantity of light removed from a beam by the role of aerosol scattering or absorption during its path [16]. Moderate Resolution Imaging Spectroradiometer (MODIS) is one of the most commonly used sensors for PM<sub>10</sub> mapping. Several studies have effectively established the relationship between MODIS derived aerosol and PM<sub>10</sub> [17]. There are 36 bands in the MODIS sensor with a wide spectral range from 0.41 to 15  $\mu$ m representing three spatial resolutions: 250 m (2 channels), 500 m (5 channels), and 1 km (29 channels). Out of these channels, the algorithm for retrieval of aerosol makes use of seven channels (0.47–2.13 $\mu$ m) to retrieve aerosol characteristics [18-23]. The MODIS aerosol retrieval algorithm for collection 5 uses three different bands for retrieval of aerosol over land, 0.47, 0.66, and 2.1  $\mu$ m. The MODIS AOD data is retrieved at 0.55  $\mu$ m. The spatial resolution for MODIS AOD is 10 km. In earlier studies, MODIS AOD is

compared with AERONET (Aerosol Robotic Network) retrieved AOD and the results show 66% match with a strong correlation of R=0.90. The quality of MODIS AOD has been evaluated for Indian subcontinent by several researchers. Jethva et al. [24] have compared the MODIS AOD and AERONET data for Kanpur site and found a high correlation of 0.91 R value. The MODIS AOD was found to be biased by Tripathi et al. [25], who compared the MODIS AOD for the same site for dust dominated season and non-dust season. In another study, MODIS AOD was applied for retrieval of PM<sub>10</sub> at Agra City, India by Chitranshi et al. [26]. The study derived that there is a weak correlation (R=0.22) of MODIS AOD with 24- hour average PM<sub>10</sub>, which was slightly improved with hourly PM<sub>10</sub> data (R=0.41). The results were significantly improved by taking the meteorological parameters for modeling PM<sub>10</sub>. By adding Relative humidity, wind speed and atmospheric temperature as independent variables resulted in highest correlation coefficient (R=0.81). A semi-physical geographically weighted regression (GWR) model for PM<sub>10</sub> mapping has been given by Zhang et al [16] for China based on MODIS AOD. The study indicates that surface RH correction on PM<sub>10</sub> and vertical correction on AOD could remarkably improve the quality of dataset for better model performance. Retrieval of PM<sub>2.5</sub> has been done using MODIS AOD in china by Lin [27]. The study is based on the characteristics of the relationship between PM<sub>2.5</sub> and aerosol characteristics like its composition and size distribution. The MODIS AOD product retrieves the data 0.55  $\mu$ m wavelength along with other channels [28].

### B. MERIS

Medium Resolution Imaging Spectrometer (MERIS) has been launched by the European Space Agency (ESA) onboard its polar orbiting Envisat Earth Observation Satellite. It is not operational now. Retalis and Sifakis [29] have done urban aerosol mapping over Athens and derived an algorithm for PM<sub>10</sub> estimation using MERIS data from ENVISAT satellite. The highest correlation was found at 0.56  $\mu$ m wavelength of MERIS band 5 for PM<sub>10</sub> distribution mapping algorithm. The correlation coefficient R-square for the PM<sub>10</sub>-AOT relationship was found to be 0.83.

### C. SPOT5

SPOT 5 is a high resolution satellite launched in 2002 and owned by Airbus Defence & Space. It collected image data at 2.5m/10m and 20m spatial resolution. SPOT-5 has been decommissioned in 2015. The SPOT 5 satellite data

was used by Tan et al. [30] for PM<sub>10</sub> mapping of Penang Island, Malaysia. Based on the reflectance of the visible wavelength bands and aerosol optical thickness (AOT), algorithm was developed for PM estimation. The atmospheric reflectance was calculated and correlation with PM<sub>10</sub> was done using regression analysis. The correlation coefficient was 0.91 for the relationship with PM<sub>10</sub> in the study area used by Tan et al. Strong linear correlation between PM<sub>10</sub> and SPOT reflectance of band 1 and band 2 has been established by the study. The spectral wavelength for band 1 is 0.50 to 0.59, and 0.61 to 0.68 for band 2 [30].

#### D. Landsat 8

PM<sub>10</sub> concentration mapping was carried out using Landsat 8 OLI data by Saleh and Hasan [31]. The correlation between PM<sub>10</sub> and Aerosol Optical Thickness (AOT) derived from satellite images using regression analysis [31, 32]. The correlation analysis shows that, among reflective bands, band 3 (Green, 0.53-0.59  $\mu\text{m}$ ) reflectance was highly correlated with ground measure PM<sub>10</sub> than the reflectance of other bands with correlation coefficient 0.80. Other than Band 3, the correlation of thermal band (band 6) was strong with R value 0.83 and was used to derive the algorithm for PM<sub>10</sub> estimation. Band 1 (0.44  $\mu\text{m}$ ) and band 2 (0.48  $\mu\text{m}$ ) can correlate with the ground station data with correlation coefficient value 0.79 and 0.78 respectively according to Saleh and Hasan findings [31].

#### E. Landsat TM

Mishra et al. [33] did Aerosol Optical Thickness (AOT) based study for Jharia coalfield, India for PM<sub>10</sub> mapping. The study has been carried out using Landsat 5 TM satellite data. The estimation was done using SWIR Landsat TM band 1 (0.45-0.52) and 2 (0.52-0.60) in which water vapour absorption is negligible. The results were verified with different ground station data and it was found to give good quality of estimation. Another study by Retalis and Sifakis (2010) also confirmed the Landsat TM derived AOT model suitable for the estimation of PM<sub>10</sub>. In a different approach by Hadjimitsis et al. [34] used pseudo-invariant targets as a tool for determining the aerosol optical thickness from Landsat 5 TM data for PM<sub>10</sub> estimation focused to area near the airport. The algorithm was applied to three Landsat-5 TM images of London Heathrow Airport area (UK) and was validated in Hellinikon Airport area (Greece). The algorithm used Landsat TM band 1 (0.45-0.52  $\mu\text{m}$ ) because water vapor and ozone absorption are considered negligible [34] [35].

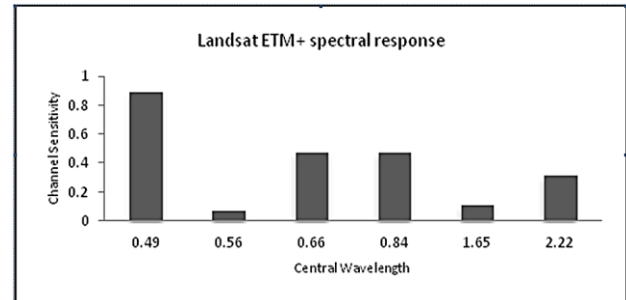


*Fig. 2 Spectral response of Landsat ETM+ channels*

#### F. Landsat ETM+

During our study, we used Landsat ETM+ due to its high resolution for PM<sub>10</sub> distribution of Vadodara city. Atmospheric correction, which is normally performed as a preprocessing step during remote sensing applications, has been effectively utilized for PM<sub>10</sub> mapping. The radiance was retrieved from the Landsat ETM+ images using the atmospheric correction to quantify the deviation of pixel values due to ambient PM<sub>10</sub>. At sensor radiance was derived using Landsat ETM+ data with surface reflectance products from USGS. The path radiance was calculated and its relationship with ground station PM<sub>10</sub> values was analyzed using correlation analysis. The results show that the approach can be effectively used for PM<sub>10</sub> estimation [36] [37].

The Principal component analysis (Fig. 2) show that Band 1 (0.49  $\mu\text{m}$ ), band 3 (0.66  $\mu\text{m}$ ) and band 4 (0.84  $\mu\text{m}$ ) has strong relationship with ground station PM<sub>10</sub> values. Regression analysis on these three bands data was performed to get PM<sub>10</sub> relationship with values calculated from satellite data. Using the results, the PM<sub>10</sub> maps were generated for the study area and validated with ground data, which show good results of PM<sub>10</sub> estimation [37].

### III. COMPARISON OF SENSORS

Table 1 shows the comparison of selected sensor characteristics. The MERIS and SPOT 5 sensors have been discontinued, but their spectral characteristics and response of different wavelength band is significant to analyze the spectral behavior of sensors with respect to wavelength region. The MODIS has 36 channels with 17 thermal channels in spectral range.

**Table 1. Comparison of selected Sensor characteristics**

Sensor	Channels	Thermal channels	Spatial resolution	Repeat cycle
MODIS	36	17	250 m / 500 m / 1 km (1 km for AOD product)	16 days
Landsat TM/ETM+	8	1	30 m / 120 m	16 days
Landsat 8	11	2	30m / 100 m	16 days
MERIS	15	None	300 m	35 days
SPOT 5	5	None	10m/ 20 m	26 days

Landsat TM/ETM+ have 7 spectral bands with 1 thermal band whereas Landsat 8 has 11 bands with 2 thermal bands. Thus, Landsat sensors have better spatial resolution than MODIS less spectral channels. Both Landsat and MODIS have 16 days repeat cycle [32].

### CONCLUSION

The knowledge and understanding of spectral characteristic is a primarily significant in remote sensing applications. PM10 estimation can be done with satellite remote sensing using various sensors. MODIS is one of the most widely used sensors due to its aerosol products availability and temporal resolution. Wide spectral resolution from 0.46 to 2.15 is used in Aerosol retrieval of MODIS, which is taken as input for Particulate Mapping in several research work done in the area of remote sensing. However, its spatial resolution is 10 km, which makes it suitable for the study of large area, but not appropriate for regional or local study. Landsat TM/ETM+ and Landsat 8 have good spatial resolution, which makes it suitable for regional and local area study. The research outcomes of the PM10 modeling show that the wavelength range of 0.45 to 0.69  $\mu\text{m}$  is highly suitable for aerosol and PM10 retrieval. Using multiple channels explains the relationship better than a single channel modeling. Adding some channel with higher wavelength (0.63-0.69  $\mu\text{m}$ ) in visible and near infrared (0.77-0.90  $\mu\text{m}$ ) region improves the results of the estimation. The studies establish that the PM10 mapping can be done without using thermal channel. However some studies have concluded that the thermal emitted energy

contributes to explain the relationship and the results can be improved by using thermal channel in the modeling. The MODIS also use band 20 (3.660 - 3.840  $\mu\text{m}$ ) for AOD product development.

### REFERENCES

- [1] B. Husar, M. Holloway, and E. Patterson, "Spatial and temporal pattern of eastern U.S. haziness: A summary," *Atmospheric Environment*, vol. 15, pp. 1919-1928, Nov 1981.
- [2] S. Ayub, and S.K. Sharma, "Particulate matter emission from thermal power plant: parent material, formation mechanism, health concerns, control devices – A Review," *Global Journal Engineering and Applied Sciences*, vol. 1, pp. 2249-2623, Jan 2000.
- [3] Zheng J., Che W., Zheng Z., Chen L., Zhong L., "Analysis of Spatial and Temporal Variability of PM10 Concentrations Using MODIS Aerosol Optical Thickness in the Pearl River Delta Region, China" *Aerosol and Air Quality Research*, vol. 13, pp. 862–876, Jan 2013.
- [4] M. Z. He, Z. Xiange, Z. Zhang and P. L. Kinney, "Fine particulate matter concentrations in urban Chinese cities, 2005-2016: A systematic review," *International Journal of environment research and public health*, vol. 14, pp. 191, Feb 2017.
- [5] S. I. Hey, "An overview of remote sensing and geodesy for epidemiology and public health application," *Advances in Parasitology*, Vol. 47, pp. 1–35, 2000.
- [6] J. L. Awange, and J. B. K. Kiema, "Fundamentals of Remote Sensing," *Environmental Geoinformatics*, pp. vol. 125, 111-118, June 2013.
- [7] W.H. Bakker, L.L.F. Janssen, and C.V. Reeves, "Principles of Remote Sensing", *The International Institute of Geo-Information Science and Earth Observation (ITC)*, Vol. 2, pp. 66-80, 2001.
- [8] S. Aggarwal, "Principles of remote sensing, Satellite Remote Sensing and GIS applications in agricultural meteorology Dehra Dun, India," *World Meteorological Organisation*, Switzerland, pp. 23–38, July 2004.

- [9] J. R. Jenson, "Remote Sensing of the Environment: An Earth Resource Perspective," Person Prentice Hall. May 2007.
- [10] J.B. Campbell, and R. H. Wynne, "Introduction to Remote Sensing," The Guilford Press, New York. Jun 2011.
- [11] T.M. Lillesand, R.W. Kiefer, and J. Chipman, "Remote Sensing and Image Interpretation," Wiley publication, New York. Jan 2015.
- [12] R.M. Hoff, and S.A. Christopher, "Remote Sensing of Particulate Pollution from Space: Have We Reached the Promised Land?," Journal of the Air & Waste Management Association, vol. 59, pp. 645-675, Oct 2009.
- [13] D. G. Streets, T. Canty, G. R. Carmichael, B. Foy, R. R. Dickerson, B. N. Duncun et al., "Emissions estimation from satellite retrievals: A review of current capability," Atmospheric Environment, vol. 77, pp. 1011-1042, May 2013.
- [14] K. A. Ali, "Remote Sensing," Laser Branch Department of Applied Sciences, University of Technology. Republic of Iraq, Ministry of Higher Education and Scientific Research. 2010.
- [15] W. P. Menzel, "Remote sensing applications with meteorological satellites," University of Wisconsin, Madison, WI. 2012.
- [16] T. Zhang, W. Gong, W. Wang, Y. Ji, Z. Zhu, and Y. Huang, "Ground Level PM<sub>2.5</sub> estimates over China using satellite based geographically weighted regression (GWR) models are improved by including NO<sub>2</sub> and enhanced vegetation index (EVI)," International Journal of environment research and public health, vol. 13, pp. 1215, Dec 2016.
- [17] G. Higgs, D. A. Sterling, S. AryL, A. Venulapalli, K. N. Priftis, and N. I. Sifakis, "Aerosol optical depth as a measure of particulate exposure using imputed censored data, and relationship with childhood asthma hospital admissions for 2004 in Athens, Greece," Environmental Health Insight, vol. 9, pp. 27-33, April 2015.
- [18] S.A. Ackerman, K.I. Strabala, W.P. Menzel, R.A. Frey, C.C. Moeller, and L.E. Gumley, "Discriminating clear sky from clouds with MODIS," Journal of Geophysical Research, vol.103, pp. 139-140, Dec 1998.
- [19] B.C. Gao, Y. J. Kaufman, D. Tanre, and R.R. Li, "Distinguishing tropospheric aerosols from thin cirrus clouds for improved aerosol retrievals using the ratio of 1.38-  $\mu\text{m}$  and 1.24  $\mu\text{m}$  channels," Geophysical Research Letters, vol. 29, pp. 1890, Sep 2002.
- [20] J. V. Martins, D. Tanre, L.A. Remer, Y.J. Kaufman, S. Mattoo, and R. Levy, "MODIS cloud screening for remote sensing of aerosol over oceans using spatial variability," Geophysical Research Letters, vol. 29, pp. 8009, Jun 2002.
- [21] R.R. Li, Y.J. Kaufman, B.C. Gao, and C.O. Davis, "Remote sensing of suspended sediments and shallow coastal waters," IEEE Transaction on Geoscience and Remote Sensing, vol. 41, pp. 559-566, March 2003.
- [22] L. A. Remer, Y. J. Kaufman, D. Tanre, S. Mattoo, D. A. Chu, J. V. Martins, R. R. Li, C. Ichoku, R. C. Levy, R. G. Kleidman, T. F. Eck, E. Vermote, and B. N. Holben, "The MODIS aerosol algorithm, products, and validation," Journal of atmospheric Science, vol. 62, pp. 947-973, April 2005.
- [23] D.G. Hadjimitsis, and C. Clayton, "Determination of aerosol optical thickness through the derivation of an atmospheric correction for short-wavelength Landsat TM and ASTER image data: an application to areas located in the vicinity of airports at UK and Cyprus," Applied Geomatics, vol. 1, pp. 31-40, May 2009.
- [24] H. Jethva, S. K. Satheesh, and J. Srinivasan, "Assessment of second-generation MODIS aerosol retrieval (Collection 005) at Kanpur, India," Geophysical Research Letters, vol. 34, pp. L19802, Oct 2007.
- [25] S. N. Tripathi, Sagnik Dey, A. Chandel, S. Srivastava, Ramesh P. Singh, and B. N. Holben, "Comparison of MODIS and AERONET derived aerosol optical depth over the Ganga Basin, India," Annales Geophysices, vol. 23, pp. 1093-1101, Jun 2005.
- [26] S. Chitranshi, S. P. Sharma, S. Dey, "Satellite-based estimates of outdoor particulate pollution (PM<sub>10</sub>) for Agra City in northern India," Air Quality, Atmosphere & Health, vol. 8, pp. 55-65, Feb 2014.

- [27] C. Lin, Y. Li, Z. Yuan, K. H. Alexis, I. C. Lau, and C. H. F. Jimmy, "Using satellite remote sensing data to estimate the high-resolution distribution of ground-level PM<sub>2.5</sub>," *Remote Sensing of Environment*, vol.156, pp. 117–128, Jan 2015.
- [28] R.C. Levy, S. Mattoo, L. A. Munchak, L. A. Remer, A. M. Sayer, F. Patadia, and N. C. Has, "The Collection 6 MODIS aerosol products over land and ocean," *Atmospheric Measurement Techniques*, vol. 6, pp. 2989–3034, Nov 2013.
- [29] A. Retalis, and N. Sifakis, "Urban aerosol mapping over Athens using the differential textural analysis (DTA) algorithm on MERIS-ENVISAT data," *ISPRS Journal of Photogrammetry and remote sensing*, vol. 65, pp. 17-25, Jan 2010.
- [30] C. E. J. Tan, H. S. Lim, C. J. Wong, M. Z. MatJafri and K. Abdullah, "A Newly Computational Intelligence Algorithm for Air Quality Mapping Using SPOT Image over Penang, Malaysia," *Fifth International Conference on Computer Graphics, Imaging and Visualisation*, Penang, pp. 389-392, 2008.
- [31] S.A.H. Saleh and G. Hasan, "Estimation of PM<sub>10</sub> Concentration using Ground Measurements and Landsat 8 OLI Satellite Image," *Journal of Remote Sensing and GIS*, vol. 3, pp. 120, April 2014.
- [32] M. Blackett, "Early Analysis of Landsat-8 Thermal Infrared Sensor Imagery of Volcanic Activity," *Remote Sensing*, vol. 6, pp. 2282-2295, March 2014.
- [33] R. K. Mishra, J. Pandey, S. K. Chaudhary, A. Khalkho, and V. K. Singh, "Estimation of air pollution concentration over Jharia coalfield based on satellite imagery of atmospheric aerosol," *International Journal of Geomatics and Geosciences*, vol. 2, pp. 723-729, Feb 2012.
- [34] D.G. Hadjimitsis, A. Retalis, and C.R.I. Clayton, "The assessment of atmospheric pollution using satellite remote sensing technology in large cities in the vicinity of airports," *Water, Air & Soil Pollution: Focus*, vol. 2, pp. 631-640, Sep 2002.
- [35] B.C. Forster, "Derivation of atmospheric correction procedures for Landsat MSS with particular reference to urban data," *International Journal of Remote Sensing*, vol. 5, pp. 799-817, March 1984.
- [36] P. Techarat, "Mapping Predictive ambient concentration distribution of particulate matter and sulfur dioxide for air quality monitoring using remote sensing," *Doctorate Thesis, Dept. of Environment Study and Engineering, University of Regina*, 2013.
- [37] A. Roy, A. Jivani, B. Parekh, "Estimation of PM<sub>10</sub> Distribution using Landsat 7 ETM+ Remote Sensing Data," *International Journal of Advanced Remote Sensing and GIS*, vol. 6, pp. 2246-2252, July, 2017.